

tion is removed. The implication is that when averaged over all Antarctica, the gravity signals from PGR and from ice variability are closely coincident (with opposing signs), and it underscores the importance of obtaining a meaningful PGR uncertainty. Our uncertainty accommodates all plausible PGR contributions, and removing even the smallest such contribution still implies a loss of ice mass.

We also determined results for WAIS and EAIS separately (Fig. 3). We estimated the errors, the leakage, and the PGR contamination of each signal, as described above for the entire ice sheet. Both these ice sheets appear to have lost mass at higher rates during 2002–2004 than during 2004–2005; this is even more evident in the total Antarctic results (Fig. 2).

By fitting a trend and annual and semiannual terms to the WAIS and EAIS results, we find that most of the Antarctic mass loss comes from WAIS. After correcting for the hydrology leakage and the PGR signal, we obtain a WAIS mass loss of $148 \pm 21 \text{ km}^3/\text{year}$. The EAIS mass loss is $0 \pm 56 \text{ km}^3/\text{year}$. Because of its relatively large uncertainty, we are not able to determine whether EAIS is in balance or not. The final error bars for WAIS and EAIS, like those for all Antarctica, are dominated by the PGR uncertainty. The predicted PGR gravity signals at individual points in WAIS are actually somewhat larger than the PGR signals at EAIS points. The overall EAIS mass error is larger than that for WAIS simply because EAIS covers an area almost three times larger, so the EAIS averaging function is sensitive to the PGR signal integrated over a much larger area.

For these individual ice sheets, but unlike for all Antarctica, the PGR and ice mass signals do not cancel one another. For EAIS, the un-

corrected GRACE trend is about equal to the PGR signal, and so we find no significant trend after removing PGR. For WAIS, the uncorrected GRACE trend and the PGR signal have about the same magnitudes but opposite signs, so the WAIS trend becomes even larger after PGR is removed.

The GRACE result for total Antarctic ice mass change includes complete contributions from such regions as the East Antarctic coastline and the circular cap south of 82°S , which have not been completely surveyed with other techniques. The comprehensive nature of this result arises because a gravity signal at the altitude of GRACE is sensitive to mass variations averaged over a broad region of the underlying surface, not just at the point directly beneath the satellite. The main disadvantage of GRACE is that it is more sensitive than other techniques to PGR; in fact, our error estimates are dominated by PGR uncertainties. As more GRACE data become available, it will become feasible to search for long-term changes in the rate of mass loss. A change in the rate would not be contaminated by PGR errors, because the PGR rates will remain constant over the satellite's lifetime.

References and Notes

1. E. Rignot, R. Thomas, *Science* **297**, 1502 (2002).
2. J. A. Church *et al.*, in *Climate Change 2001: The Scientific Basis*, Third Assessment Report of the IPCC (Cambridge Univ. Press, Cambridge, 2001), pp. 639–694.
3. C. Davis, Y. Li, J. J. McConnell, M. Frey, E. Hanna, *Science* **308**, 5730 (2005).
4. R. Thomas *et al.*, *Science* **306**, 255 (2004).
5. GRACE, launched in March 2002 and administered by NASA and the Deutsches Zentrum für Luft-und Raumfahrt, is mapping Earth's gravity field every 30 days during its 10- to 11-year lifetime. GRACE consists of two identical satellites in identical orbits, separated by $\sim 220 \text{ km}$. The

satellites use microwaves to monitor their separation distance. Onboard accelerometers and Global Positioning System receivers detect nongravitational accelerations and geocentric orbital motion.

6. M. Cheng, B. Tapley, *J. Geophys. Res.* **109**, B09402 (2004).
7. J. Wahr, S. Swenson, V. Zlotnicki, I. Velicogna, *Geophys. Res. Lett.* **31**, L11501 (2004).
8. B. Tapley, S. Bettadpur, M. Watkins, C. Reigber, *Geophys. Res. Lett.* **31**, L09607 (2004).
9. I. Velicogna, J. Wahr, *Geophys. Res. Lett.* **32**, L18505 (2005).
10. M. Tamisiea, E. Leuliette, J. Davis, J. Mitrovica, *Geophys. Res. Lett.* **32**, L20501 (2005).
11. S. Swenson, J. Wahr, P. C. D. Milly, *Water Resour. Res.* **39**, 1223 (2003).
12. To determine the scaling factor for the entire ice sheet, we applied our averaging function to the gravitational signature of a uniform 1-cm water mass change spread evenly over the ice sheet. We obtained an estimate of 0.62 cm. We thus multiplied each GRACE estimate by 1/0.62. Determining scaling factors for WAIS and EAIS is more complicated because the EAIS averaging function extends slightly over WAIS and vice versa. We applied each averaging function to a uniform mass change over each region individually and used the four resulting values to determine the linear combination of WAIS and EAIS results that correctly recovers the mass in each region.
13. J. Wahr, S. Swenson, I. Velicogna, *Geophys. Res. Lett.*, in press.
14. M. Rodell *et al.*, *Bull. Am. Meteorol. Soc.* **85**, 381 (2004).
15. T. Lee, I. Fukumori, D. Menemenlis, Z. Xing, L. Fu, *J. Phys. Oceanogr.* **32**, 1404 (2002).
16. W. R. Peltier, *Annu. Rev. Earth Planet. Sci.* **32**, 111 (2004).
17. E. Ivins, T. S. James, *Antarct. Sci.* **17**, 541 (2005).
18. I. Velicogna, J. Wahr, *J. Geophys. Res.* **107**, 2376 (2002).
19. We thank S. Bettadpur, J. Cheng, J. Reis, E. Rignot, and M. Watkins for data and advice. This work was supported by NASA's Cryospheric and Solid Earth Programs and by the NSF Office of Polar Programs. This research was partially carried out at the Jet Propulsion Laboratory.

13 December 2005; accepted 21 February 2006

Published online 2 March 2006;

10.1126/science.1123785

Include this information when citing this paper.

Seasonality and Increasing Frequency of Greenland Glacial Earthquakes

Göran Ekström,^{1*} Meredith Nettles,² Victor C. Tsai¹

Some glaciers and ice streams periodically lurch forward with sufficient force to generate emissions of elastic waves that are recorded on seismometers worldwide. Such glacial earthquakes on Greenland show a strong seasonality as well as a doubling of their rate of occurrence over the past 5 years. These temporal patterns suggest a link to the hydrological cycle and are indicative of a dynamic glacial response to changing climate conditions.

Continuous monitoring of seismic waves recorded at globally distributed stations (1) has led to the detection and identification of a new class of earthquakes associated

with glaciers (2, 3). These “glacial earthquakes” are characterized by emissions of globally observable low-frequency waves that are incompatible with standard earthquake models for tectonic stress release but can be successfully modeled as large and sudden glacial-sliding motions (4). Seismic waves are generated in the solid earth by the forces exerted by the sliding ice mass as it accelerates down slope and subsequently decelerates. The observed duration

of sliding is typically 30 to 60 s. All detected events of this type are associated with mountain glaciers in Alaska or with glaciers and ice streams along the edges of the Antarctic and Greenland ice sheets. The Greenland events are most numerous, and we present new data indicating a strong seasonality and an increasing frequency of occurrence for these events since at least 2002.

For the period January 1993 to October 2005, we have found 182 earthquakes on Greenland by analysis of continuous records from globally distributed seismic stations (5). None of these earthquakes are reported in standard seismicity catalogs. We have modeled seismograms for 136 of the best-recorded events to confirm their glacial-sliding source mechanism and obtain improved locations (Fig. 1) (6, 7). This analysis yields an estimate of the twice-time-integrated active force couple at the earthquake source, a quantity that can be interpreted as the product of sliding mass and sliding distance (2, 8). All events have long-period seismic magnitudes in the range 4.6 to 5.1, corresponding to a product

¹Department of Earth and Planetary Sciences, Harvard University, 20 Oxford Street, Cambridge, MA 02138, USA.

²Lamont-Doherty Earth Observatory of Columbia University, Palisades, NY 10964, USA.

*To whom correspondence should be addressed. E-mail: ekstrom@seismology.harvard.edu

of sliding mass and sliding distance of 0.1 to 2.0×10^{14} kg m. The locations resulting from our seismogram modeling have an uncertainty of approximately 20 km. All 136 earthquakes analyzed can be spatially associated with major outlet glaciers of the Greenland Ice Sheet (Fig. 1).

We investigate the seasonality of the glacial earthquakes by counting the number of events occurring in each month over the 12-year period 1993 to 2004. Greenland earthquakes occur in each month of the year but are more frequent during the late summer months (Fig. 2A). Seasonal variations in background seismic noise, with higher noise levels during winter months, may influence the detection of seismic events.

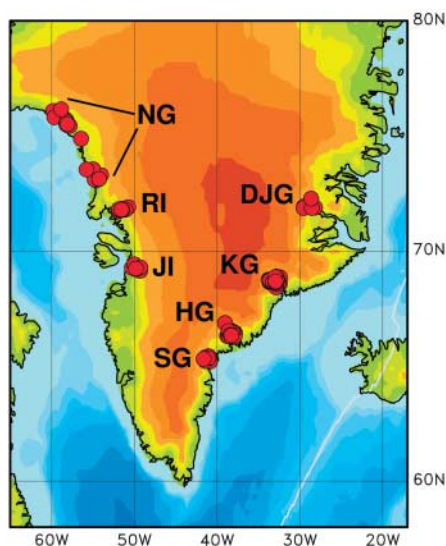


Fig. 1. Topographic map of southern Greenland and vicinity. The locations of 136 glacial earthquakes defining seven groups are indicated with red circles: DJG, Daugaard Jensen Glacier (5 events); KG, Kangerdlugssuaq Glacier (61); HG, Helheim Glacier (26); SG, southeast Greenland glaciers (6); JI, Jakobshavn Isbrae (11); RI, Rinks Isbrae (10); NG, northwest Greenland glaciers (17). Owing to the tight clustering of the earthquakes, many of the individual symbols on the map overlap.

A control group consisting of standard (non-glacial) earthquakes located north of 45°N , detected by the same method and in the same magnitude range as the glacial earthquakes (4.6 to 5.1), displays no seasonality, indicating that variations in the detection threshold are not the cause of the observed behavior (9, 10). Summer surface melting followed by transport of meltwater to the glacier base and the consequent lowering of the effective friction at the base provide a plausible explanation for the seasonal signal (11, 12). However, the occurrence of events during the coldest months of the year suggests that the influx of water accelerates the events rather than controls them.

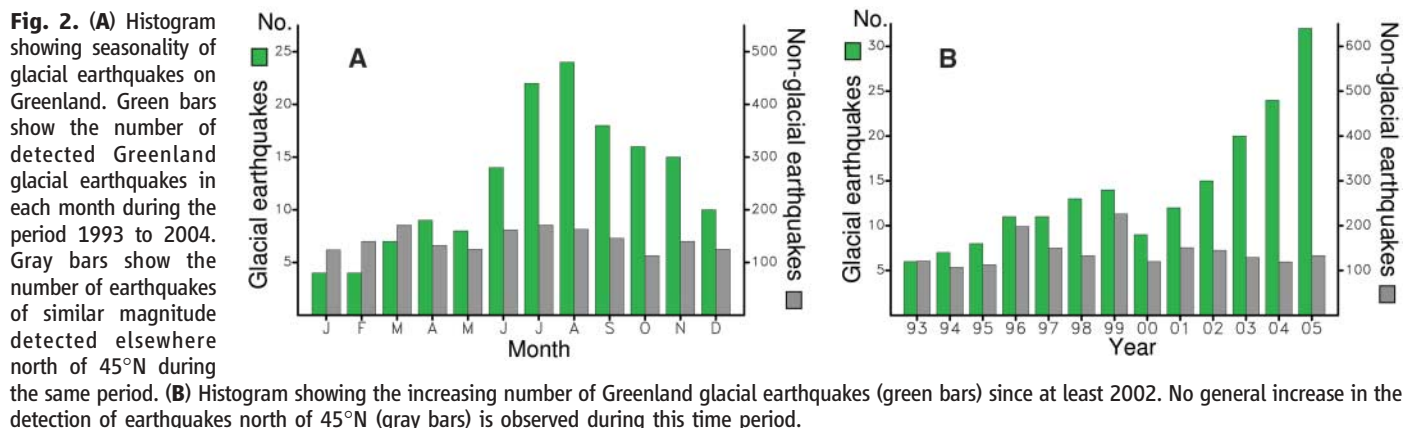
Summer melting of the Greenland Ice Sheet has become more widespread during the past decade (13), and many outlet glaciers have thinned, retreated, and accelerated during the same time period (14–19). We investigate temporal changes in the frequency of Greenland glacial earthquakes by counting events for each year since 1993 (Fig. 2B). Detections for 2005 are for January to October and are based on the subset of seismic data available in near-real time. A clear increase in the number of events is seen starting in 2002. To date in 2005, twice as many events have been detected as in any year before 2002. The control group of detected events was used to determine whether an improvement in the detection capability of the seismic network could explain the observed increase (9). No clear trend is seen in the number of control events detected, indicating that the observed increase in the number of glacial earthquakes is real.

Recent evidence suggests that ice sheets and their outlet glaciers can respond very quickly to changes in climate, primarily through dynamic mechanisms affecting glacier flow (12, 15). The seasonal signal and temporal increase apparent in our results are consistent with a dynamic response to climate warming driven by an increase in surface melting and the supply of meltwater to the glacier base. The number of events detected at each outlet glacier using the global seismic network is relatively small, and it is therefore difficult to draw robust conclusions about behavior at any single glacier. However, both the seasonal and temporal patterns reported here are observed for independent subsets of the data corresponding to east and west Greenland. The increase in number of glacial earthquakes over time thus appears to be a response to large-scale processes affecting the entire ice sheet. We note also that a part of the increase in the number of glacial earthquakes in west Greenland is due to the occurrence of more than two dozen of these earthquakes in 2000 to 2005 at the northwest Greenland glaciers, where only one event (in 1995) had previously been observed.

Understanding the mechanisms of the dynamic response of ice sheets to climate change is important in part because ice-sheet behavior itself affects global climate, through, for example, the modulation of freshwater input to the oceans (20). Glacial earthquakes represent one mechanism for the dynamic thinning of outlet glaciers, providing for the transport of a large mass of ice a distance of several meters (e.g., 10 km^3 by 10 m) over a duration of 30 to 60 s. Although the mechanics of sudden sliding motions at the glacier base are not known, the seasonal and temporal patterns reported here suggest that the glacial earthquakes may serve as a marker of ice-sheet response to external forcing. Continuous monitoring of ice velocity at outlet glaciers, along with regional seismic monitoring, would provide important insight into the nature of the dynamic response of ice sheets to changes in climate.

References and Notes

1. R. Butler *et al.*, *EOS* **85**, 225 (2004).
2. G. Ekström, M. Nettles, G. A. Abers, *Science* **302**, 622 (2003).
3. G. Ekström, *Bull. Seismol. Soc. Am.*, in press.
4. Seismograms from the glacial earthquakes are predicted poorly by standard faulting models in which the earthquake source is represented by a moment tensor or a double-couple force system. The seismic data are explained well by a single-force system like that used to describe landslide sources (2, 8).
5. Initial detections and locations of the glacial earthquakes are obtained by array analysis of continuous seismic data (1), using a set of globally distributed test locations that allows for earthquake epicenters to be determined on a 0.5°



by 0.5° grid. The quality of each detection and location is assessed based on the correlation between the observed signal envelope and that predicted for the selected location (2, 3). Only events with high-quality detections are discussed in this report.

6. V. C. Tsai, G. Ekström, *EOS* **86**, Abstract C43A-02 (2005).
7. The earthquakes were analyzed by centroid-single-force (CSF) inversion (2, 8) to obtain estimates of the best fitting source parameters, including the centroid location, time, size, and direction of sliding for each event.
8. H. Kawakatsu, *J. Geophys. Res.* **94**, 12,363 (1989).
9. The control group consists of all detected events north of 45°N that are not identified as glacial earthquakes on Greenland. Of this group of 1832 events, 98% are also found in standard earthquake catalogs. The remaining 35 events occur in seismically active areas and are also likely to be standard earthquakes. The observed rate of regular tectonic earthquakes at high northern latitudes, a proxy for detection-threshold stability, shows neither seasonality nor a temporal trend.
10. Although the glacial earthquakes discussed here have defining characteristics (including size, geometry, and duration) that distinguish them from other types of seismic events associated with glaciers, seasonality has been observed in calving-related glacial microearthquake activity in previous studies, for example, at Columbia Glacier, Alaska (21).
11. M. Meier *et al.*, *J. Geophys. Res.* **99**, 15,219 (1994).
12. H. J. Zwally *et al.*, *Science* **297**, 218 (2002).
13. K. Steffen, S. V. Nghiem, R. Huff, G. Neumann, *Geophys. Res. Lett.* **31**, L20402, 10.1029/2004GL020444 (2004).
14. I. Joughin, W. Abdalati, M. Fahnestock, *Nature* **432**, 608 (2004).
15. W. Krabill *et al.*, *Geophys. Res. Lett.* **31**, L24402, 10.1029/2004GL021533 (2004).

16. A. Luckman, T. Murray, *Geophys. Res. Lett.* **32**, L08501, 10.1029/2005GL023813 (2005).
17. I. M. Howat, I. Joughin, S. Tulaczyk, S. Gogineni, *Geophys. Res. Lett.* **32**, L22502, 10.1029/2005GL024737 (2005).
18. G. S. Hamilton, L. A. Stearns, *EOS* **86**, Abstract C23A-1159 (2005).
19. E. Rignot, *EOS* **86**, Abstract C41A-02 (2005).
20. P. U. Clark, R. B. Alley, D. Pollard, *Science* **286**, 1104 (1999).
21. A. Qamar, *J. Geophys. Res.* **93**, 6615 (1988).
22. Supported by National Science Foundation grants EAR-0207608 and OPP-0352276 and a National Science Foundation Graduate Fellowship (V.C.T.). The seismic data were collected and distributed by the Incorporated Research Institutions for Seismology and the U.S. Geological Survey.

1 November 2005; accepted 9 January 2006
10.1126/science.1122112

The Preparation and Structures of Hydrogen Ordered Phases of Ice

Christoph G. Salzmann,^{1,2*} Paolo G. Radaelli,^{3,4} Andreas Hallbrucker,¹ Erwin Mayer,¹ John L. Finney⁴

Two hydrogen ordered phases of ice were prepared by cooling the hydrogen disordered ices V and XII under pressure. Previous attempts to unlock the geometrical frustration in hydrogen-bonded structures have focused on doping with potassium hydroxide and have had success in partially increasing the hydrogen ordering in hexagonal ice I (ice Ih). By doping ices V and XII with hydrochloric acid, we have prepared ice XIII and ice XIV, and we analyzed their structures by powder neutron diffraction. The use of hydrogen chloride to release geometrical frustration opens up the possibility of completing the phase diagram of ice.

Water molecules in all of the 12 known crystalline phases (Fig. 1) are tetrahedrally hydrogen bonded to four neighbors. A consequence of this connectivity is that individual water molecules may adopt, in principle, six different orientations. In ice structures, the Bernal Fowler rules (1, 2) require that one hydrogen atom participates in each hydrogen bond. Therefore, the orientation of a given molecule is restricted by its local environment and cannot rotate to another hydrogen-bonded orientation without its neighbors also reorienting. In spite of these restrictions, a very large number of nearly degenerate molecular configurations, which are all related to each other by cooperative reorientation, exist near the true ground state. This is a consequence of the inherent geometrical frustration of the ice lattice, a particularly interesting aspect of these hydrogen-bonded systems that is relevant for other geometrically frustrated systems such as

protein folding and neural networks (3, 4). Furthermore, there are important parallels with frustrated magnetic systems (5), which themselves have been called “spin ices.”

At high temperatures, water ices can explore their configurational manifold thanks to the presence of mobile point defects, which locally lift the constraints of the geometrical frustration (6–8). The two types of thermally induced point defects uniquely found in ices are rotational defects, in which either two (D defect) or no hydrogen atoms (L defect) are found between neighboring oxygen atoms, and ionic defects

(H₃O⁺ and OH[−]) (6). These defects can migrate along chains of molecules through the crystal structure leaving reoriented molecules behind them, thus providing the mechanism for collective reorientation in ice. The molecular orientations found in the high-temperature, liquidus phases of ice (Ih, III, IV, V, VI, VII, and XII) are more or less random, so that the space-time averaged structure of those phases is hydrogen disordered (6, 7, 9, 10). As the temperature is lowered, the tendency to occupy the energetically most favored orientations increases. However, for most phases, this ordering process is hampered by the decreasing number density and mobility of the point defects. Except for disordered ices III and VII, intrinsic point defects are not sufficient to facilitate phase transitions from the hydrogen disordered phases, including ice V (7, 9, 11–13) or ice XII (10, 14, 15), to their energetic (hydrogen ordered) ground-state phases. Instead, ergodicity is lost before the long-range ordering transition, and the hydrogen disordered structures are frozen-in. For this reason, the hydrogen ordered ground states of ices V and XII remain undiscovered so far.

Point defects can also be introduced by doping ices with impurities. However, the effectiveness of each particular dopant to pre-

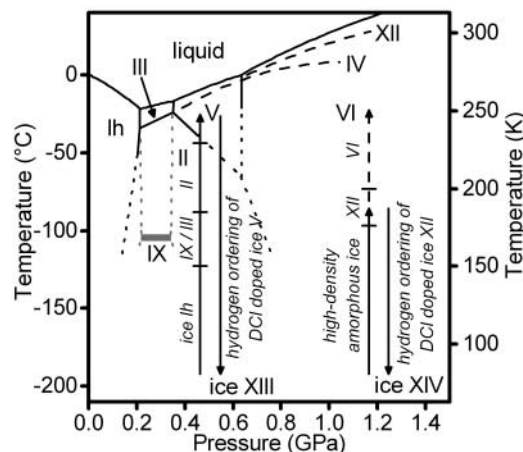


Fig. 1. The phase diagram of ice, including liquidus lines of metastable ices IV and XII (long dashed lines) and extrapolated equilibria lines at low temperatures (short dashed lines). The pathways of preparation of DCI-doped ices V and XII are indicated by arrows. Ice V was produced by isobarically heating ice Ih to 250 K at 0.5 GPa. Pure ice XII was crystallized from high-density amorphous ice by isobaric heating at 1.2 GPa at 11 K min^{−1} to 190 K, which is 10 K below the temperature where transition to more stable ice VI would occur. Both ice V and ice XII can be handled at ambient pressure up to temperatures of ~150 K, where conversion to cubic ice Ic occurs (19, 20).

¹Institute of General, Inorganic, and Theoretical Chemistry, University of Innsbruck, Innrain 52a, 6020 Innsbruck, Austria.

²Inorganic Chemistry Laboratory, University of Oxford, South Parks Road, Oxford OX1 3QR, UK. ³ISIS Facility, Rutherford Appleton Laboratory, Council for the Central Laboratory of the Research Councils (CLRC), Chilton, Didcot OX11 0QX, UK. ⁴Department of Physics and Astronomy, University College London, Gower Street, London WC1E 6BT, UK.

*To whom correspondence should be addressed. E-mail: christoph.salzmann@chemistry.oxford.ac.uk

Seasonality and Increasing Frequency of Greenland Glacial Earthquakes

Göran Ekström, Meredith Nettles and Victor C. Tsai

Science **311** (5768), 1756-1758.
DOI: 10.1126/science.1122112

ARTICLE TOOLS

<http://science.sciencemag.org/content/311/5768/1756>

PERMISSIONS

<http://www.sciencemag.org/help/reprints-and-permissions>

Use of this article is subject to the [Terms of Service](#)

Science (print ISSN 0036-8075; online ISSN 1095-9203) is published by the American Association for the Advancement of Science, 1200 New York Avenue NW, Washington, DC 20005. 2017 © The Authors, some rights reserved; exclusive licensee American Association for the Advancement of Science. No claim to original U.S. Government Works. The title *Science* is a registered trademark of AAAS.